Chapter 18
Neural Field Dynamics and the Evolution of the Cerebral Cortex

James J. Wright and Paul D. Bourke

Abstract We describe principles for cortical development which may apply both to the evolution of species, and to the antenatal development of the cortex of individuals. Our account depends upon the occurrence of synchronous oscillation in the neural field during embryonic development, and the assumption that synchrony is linked to cell survival during apoptosis. This leads to selection of arrays of neurons with ultra-small-world characteristics. The "degree of separation" power law is supplied by the combination of neuron sub-populations with differing exponential axonal tree distributions, and consequently, in the visual cortex, connections emerge in anatomically realistic patterns, with an ante-natal arrangement which projects signals from the surrounding cortex onto each macrocolumn, in a form analogous to the projection of a Euclidean plane onto a Möbius strip. Simulations of signal flow explain cortical responses to moving lines as functions of stimulus velocity, length and orientation. With the introduction of direct visual inputs, under the operation of Hebbian learning, development of mature selective response "tuning" to stimuli "features" then takes place, overwriting the earlier ante-natal configuration. Further assuming similar development principles apply to inter-areal interactions in the developing cortex, a general principle for the evolution of increasingly complicated sensory-motor sequences, at both species-evolution and individual time-scales, is implicit.

J.J. Wright (✉)
Faculty of Medicine, Department of Psychological Medicine, University of Auckland, Auckland, New Zealand

P.D. Bourke
iVEC@UWA, University of Western Australia, Perth, WA, Australia

AQ1

S. Coombes et al. (eds.), *Neural Fields*, DOI 10.1007/978-3-642-54593-1_18,

18.1 Introduction

This chapter outlines the wider biological motivation of recent work from our group, in which we have applied neural field theory to the embryological development of the primary visual cortex. The embryogenesis of brains appears to mirror the phylogenetic history of the brains of antecedent species, and neurodevelopment and later learning must, throughout life, take place hand-in-hand. So, perhaps it will be of value to consider neuron dynamics within this evolutionary and developmental context? This idea is hardly new—in relation to neural networks it can be traced back through Hebb [42] to William James [50], and beyond. In its anatomical aspects, it is given its strongest evolutionary context in the works of Papez [76], Yakovlev [109], Sperry [88], and MacLean [57, 69]. In these latter works, the process of encephalization was explained in terms of the drive toward ever more neurons, and of the advantages of envelopment of the "older" (species') brain within the "newer" brain, thus providing centripetal/centrifugal control and supervisory functions, so that the function of hard-wiring circuits was not lost as progressively flexible "new" circuits were added, at paleo-cortical, and then neo-cortical level. Two corollary aspects of this evolutionary sequence have been less emphasised, but seem also to be important. The first aspect seems almost too obvious to require stating—the developing neural organization must retain, as cortical size increases, a primary capacity to convert information delivered to the sensory cortices into motor outputs, beginning from simple sensory-motor systems exemplified by the tadpole tectum [45]. Perhaps less obviously, it seems that there must be a modular principle for sensory-motor conversions signal conversions, such that new pieces of cortex can be "inserted", without disruption of antecedent functions. The latter aspect has gained in importance since the classic works of MacLean and his precursors. As encephalization increases, there is are corollary demands to minimize information transfer times and physical size, while maximizing total synaptic connectivity and total information storage capacity, all the while minimizing metabolic demand as much as possible. In approaching an optimum neuronal assembly, there is a synergy between the need to maximize connectivity, minimize connection distances, and maximize information storage capacity, for the following reason: as encephalization increases, the small neurons of small, primitive creatures give way to long, attenuated neurons of large, advanced creatures. This increases the connectivity of each neuron, and is compatible with an efficient connection system among the neurons, for which some "ultra-small-world" arrangement [21] would be optimal. The tendency toward attenuation of neurons has a limit at which the neuron, described as a fractal object, approaches a dimension of three—i.e., as large a surface area of synaptic contacts as possible, for as small a cell volume as possible. Assuming the supply of metabolites is subject to some upper practical limit, there must also result an increasing competition for crucial metabolites among synapses. There is good evidence that competition between synapses for resource takes place at a number of anatomical sites (e.g., [7, 40, 51, 61, 74]). If there was only enough critical metabolite for half the synapses to operate at maximum capacity, then, as

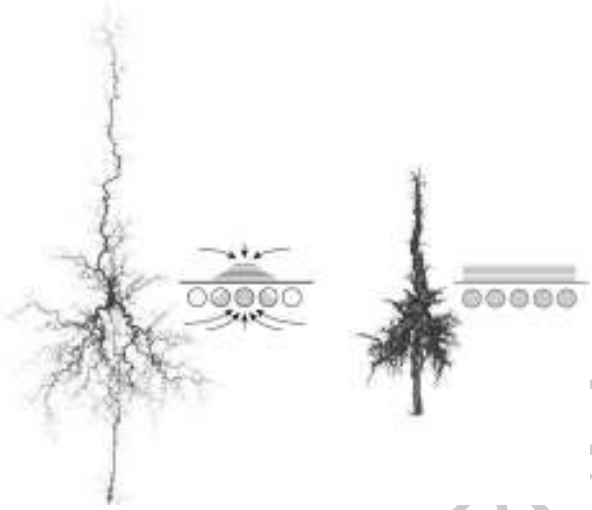

Fig. 18.1 Surface-to-volume ratios of dendrites, and competition for critical metabolites. Attenuated dendrites of a neuron with fractal dimension approaching three (*left*), are contrasted with less attenuated dendrites of a neuron with fractal dimension markedly less than three (*right*). To the right of each neuron, synapses and post-synaptic membranes are represented schematically. For the more "developed" neuron, where cell surface to volume is high, *arrows* indicate the flow of a critical metabolite away from inactive synapses to active synapses, induced by demand—a competition that need not take place when dendritic surface area is relatively reduced

well as generating a maximum of synapses, attenuation plus competition could maximize the possible Shannon entropy of the synaptic states, by maximizing the complexity of possible neural signal pathways among the neurons (See Fig. 18.1). If variation of the supply of metabolites fluctuates with firing states of the network, and there are a multiplicity of critical factors, and consequently of time-scales of their supply, conditional Markov processes of great complexity are possible, from which ensemble those beneficial to survival must be selected.

Since "ontogeny recapitulates phylogeny", and the considerations above have determined the pathway followed by species-level natural selection, then what is their analogue during individual development? During embryogenesis there is a further happy convergence of effects, which at first seem antagonistic. The active firing of the neurons, which seems to add a burden of metabolic demand to the developing cells may assist the avoidance of cell-death by apoptosis, and may do so in a way which leads to an efficient primary organizational underpinning, for the learning of ever-more complicated sensory-motor sequences in post-natal life. We next sketch relevant background findings, before presenting application of these principles to problems of development of the primary visual cortex (V1). We have concentrated on the primary visual cortex because of the wealth of experimental data that has been gathered in that cortical area, but we intend our treatment to be more general, and applicable to the cortex more widely, as is later described.

18.1.1 Genetic Expression, Cell Firing and Apoptosis in Cortical Development

The emergence of functional neuronal organization and connectivity in the developing cerebral cortex depends on differentiation, proliferation and migration of neurons [44]. Early, thalamus-independent (i.e., sensory-pathway-independent) steps in the process of cortical arealization take place on the basis of information intrinsic to the cells, as proposed by Rakic in his protomap hypothesis [78]. It is these genetic programmes that lead to the characteristic cellular shapes of different populations of neurons during the stages of cell differentiation. However, factors not simply explained by direct gene expression in the cells seem to be important. action potential generation is present from early embryonic development (e.g., [5]) and plays a part in the development of cortical microcircuitry [110]. As cell differentiation proceeds, programmed cell death plays a major role. Fragmented nuclear DNA markers suggest that the bulk of differentiating neurons die soon after they are generated, and the majority of the cells that die are in the fastest proliferating regions [12]. Cell firing itself is not essential to synaptic development, since cultured neurons blocked from generating action potentials by xylocaine continue to develop synapses [65]. Yet, although the generation of action potentials must greatly increase metabolic demands, synchronous action potential generation appears to protect against apoptosis, since neurons in neonatal cerebral cortical slices show increased apoptosis when their capacity to enter into synchronous firing is disrupted by pharmacological means [43]. Embryonic neurons developing in vitro develop synchronous firing, and as their growth proceeds, also show self-organization into "small world" networks [22].

We propose that synchronous firing and protection from apoptosis are related because competition among developing neurons and synapses, although mediated by trophic factors [39,94,97,98], is ultimately a competition for available metabolic energy, and that pulse synchrony increases uptake of critical metabolic resources, perhaps by some collective pumping action. Consequently, cell groups interlinked in such a way as to fire in maximum synchrony can supply themselves with sufficient resource to survive, while others cannot.

18.1.2 Cell Firing and Synchronous Oscillation

synchronous oscillation of pulses and local field potentials is a ubiquitous aspect of cortical activity [16,26,27,37,87] and has been proposed as a solution to the "binding problem" of perceptual grouping and cognitive processing [27,87]. Synchrony is not absolute, but refers to occurrence of maximum cross-correlation at zero lag, and is a broadband phenomenon in the temporal frequency domain [16]. Detailed models of synchronous firing in specific cell assemblies [26, 83, 87, 89, 95, 100] do not explain the synchrony seen in neuron cultures, brain slices, or the early foetal brain.

A more fundamental mechanism, that is a universal property of networks with summing junctions including dendrites [20,80,107] is applicable, however, and also appears in simulations that also accurately reproduce spectra, cross-correlations and excitatory/inhibitory timings characteristic of activated cortex [104, 105]. In these simulations synchrony results from interaction of waves travelling in opposite directions, and increases in amplitude toward an ideal steady-state in which there is sustained symmetrical exchange of signals between all excitatory neurons [105], associated with concurrent local excitatory/inhibitory oscillation. That is, synchrony reflects an oscillatory steady-state with bidirectional equality of signal exchange. Unidirectional traveling waves are transient deviations from that equilibrium of exchange.

18.1.3 Unresolved Issues in the Development of V1

18.1.3.1 The Geometry of Response Organization

Since the discovery that individual cells in V1 respond with an orientation preference (OP) to visual lines of differing orientation [48], attempts to analyze the response organization and explain its relationship to cortical function [92, 99, 102] have played a pivotal role in neuroscience. The surface organization of OP in V1 has recently been compared with appropriate random surrogates, and shown, in some species at least, to approximate an hexagonal rotational periodicity in which each roughly delineated macrocolumnar unit exhibits all values of OP arrayed around a pinwheel [68, 75]. Varying chirality and orientation of the pinwheels achieves continuity of OP at the columnar margins, thus producing linear zones and saddles. In any individual, irregular variation from the average periodicity occurs, and some species—particularly those with smaller brains and hence visual cortices—exhibit little or no sign of this ordering. Because of this marked interspecies variation, serious doubt has been expressed that the pattern is of functional significance at all, since response maps are absent in some species without those species having any apparent deficit in vision [47].

18.1.3.2 The Superficial Patch System

A further puzzle of intracortical V1 organization is posed by the superficial patch system. This system, composed of relatively long-range, largely excitatory [46, 59] patchy connections [35, 81] is ubiquitous in cortex [67] and has a functional relationship to OP. Patchy connections develop before sensory afferents reach the cortex [18,23,77,82] and do not arise or terminate in the vicinity of OP singularities. They link areas of common OP ("like-to-like") over distances several times the diameter of a macrocolumn [17, 36, 63, 68], are periodic on roughly the same interval as OP, and are largely patch-reciprocal [4, 81]. Just as for maps of response properties, there is variation of patchy connection orderliness between species [68].

18.1.3.3 Model Characterization of Primary Feature Responses

Explanation of organization of OP has been attempted in a group of now-classical theories, which we will refer to as "standard models", following the comparative description of Swindale [92]. Dimension reduction methods [24, 25, 52] show that the response maps of OP, eye preference (OC), direction preference (DP) and spatial frequency preference (SF) are consequences of requiring continuity and completeness of representation of each response property, in a two-dimensional representation in which every type of response property occurs within any small area on the surface of V1 [19, 92]. The same ordering can also be explained as a consequence of competitive Hebbian learning among small neighborhood assemblies of excitatory neurons [38]. All standard models depend on seeding with oriented lines, in one way or another [24, 38, 64, 70, 71, 90, 91, 93, 99] and otherwise similar models avoiding this limitation do not accurately reproduce response maps [54–56, 60]. Initial belief that response to simple oriented lines in the visual field formed the basis of OP maps has been undermined in two ways. Firstly, maps of OP appear in the cortex prior to visual experience [11, 85, 101], and although it is argued that structured stimuli may arise from retinal inputs in the absence of visual experience [1, 75, 79], the absence of particular visual stimuli in the post-natal environment eliminates subsequent neural response to those stimuli [10] indicating that direct visual experience is essential at some stage. Secondly, and more recently, Basole and colleagues, who tested OP using stimulus lines moving at different speeds, and oriented at differing angles to the line of movement of the stimulus, found OP to be a function of these variables to such a degree that for lines oriented non-orthogonally to the direction of movement, OP could vary progressively with increments of speed to an asymptotic limit of 90° [8, 9]. This effect was attenuated for lines of progressively greater length.ă Standard models could not account for these effects, and to salvage the standard models in essence, if not specifics, subsequent workers explained these results by considering the temporal and spatial frequencies associated with the moving stimuli. Issa and colleagues [6, 49] showed responses to specific features could be explained by fitting six parameters—OP, SF preference, and temporal frequency preference, and the tuning bandwidths of all three. This description is referred to as the spatio-temporal filter model. ă

18.2 Developmental Synergy of Apoptosis and Synchrony, Applied to V1

Wright and Bourke (2013, A model for embryogenesis of cortical macrocolumns and superficial patchy connections: consequent neuronal responses at maturity, unpublished manuscript) [106] used a generic form of neural field equations for an idealised, isotropic, neural field, within which individual neurons are embedded. This represents the developing cortex's potential isotropic connections, from which

actual connections are selected during development, by the combined unfolding of genetic cascades, and of apoptosis. The scale of the field is that of a cortical area such as V1, representing intracortical connections rather than cortico-cortical. Thus, the density of connection between neurons declines with increasing separation of their cell bodies [15]. The high non-linearity of synapto-dendritic summations are linearized at the field level, and axonal conduction speed is considered single-valued. Subject to these strictures, these general equations include the minimum relevant features:

$$\varphi_p^{\mathbf{qr}'}(t) = f_p^{\mathbf{qr}'} \times Q_p\left(\mathbf{r}', t - \frac{|\mathbf{q}-\mathbf{r}'|}{v}\right) \tag{18.1}$$

$$\psi_p^{\mathbf{qr}'}(t) = M_p^{\mathbf{qr}'}(t) * \varphi_p^{\mathbf{qr}'}(t) \tag{18.2}$$

$$\Psi_p(\mathbf{q}, t) = \int_D \psi_p^{\mathbf{qr}'}(t)\, \mathrm{d}\mathbf{r}' \tag{18.3}$$

$$V_p(\mathbf{q}, t) = G_e(t) * \Psi_e(\mathbf{q}, t) + G_i(t) * \Psi_i(\mathbf{q}, t) \tag{18.4}$$

$$Q_p(\mathbf{q}, t) = f_\Sigma(V_p(\mathbf{q}, t)) + E_p(\mathbf{q}, t)\,. \tag{18.5}$$

Subscript $p \in \{e, i\}$ refers to excitatory or inhibitory neurons; superscript $\mathbf{qr}'$ refers to synaptic connection from $\mathbf{r}'$ to $\mathbf{q}$ where $\mathbf{q}, \mathbf{r}'$ are cortical positions in domain D, occupied by single neurons. $\varphi_p^{\mathbf{qr}'}(t)$ is the flux of pulses reaching presynapses at the neuron at $\mathbf{q}$, from the neuron at $\mathbf{r}'$. $\psi_p^{\mathbf{qr}'}(t)$ is the synaptic current generated by $\varphi_p^{\mathbf{qr}'}(t)$. $\Psi_p(\mathbf{q}, t)$ is the aggregate synaptic current of type p generated at $\mathbf{q}$. $V_p(\mathbf{q}, t)$ is the soma membrane potential (relative to the resting potential) generated at $\mathbf{q}$. $Q_p(\mathbf{q}, t)$ is the pulse emission rate at $\mathbf{q}$. $f_p^{\mathbf{qr}'}$ is the probability density of occurrence of presynapses generated by axons of the neuron at $\mathbf{r}'$ terminating at $\mathbf{q}$. v is axonal conduction speed. $M_p^{\mathbf{qr}'}(t)$ is the impulse response function transforming presynaptic flux to synaptic current. $G_p(t)$ is the impulse response function transforming presynaptic flux into dendritic potentials. $f_\Sigma(V_p(\mathbf{q}, t))$ is a sigmoid function describing the local conversion of dendritic potentials into the rate of generation of action potentials. $E_p(\mathbf{q}, t)$ is a driving signal noise, arising from intrinsic random cell action potentials.

Restriction of the field to the scale of a cortical area carries several implications, all because the probability of connections between any two neurons declines with distance of separation. Firstly, descriptively we can consider "reciprocal couplings" as an idealization/representation of field coupling symmetry, and in some instances reciprocal couplings will in fact exist. Secondly because of more generally dense connections among near neighbours, smoothing at dendritic summation requires that $Q_p(\mathbf{q}, t)$ is spatially and temporally "brown"—i.e., has high correlation at short distances and times of separation. Thirdly, in the sparsely connected network, the average "degree" of separation—i.e., the average number of neighboring cells traversed by synaptic connections linking one cell to another—will also increase in proportion to physical distance of separation.

A further crucial property upon which our results depend is the occurrence of gamma oscillation in the cortical field, when the cortex is sufficiently excited, as occurs in the developing mammalian cortex in later foetal development [58, 62]. Experimental observations [32,33,41] show intrinsic cortical oscillation arises from alternating excitatory cell and inhibitory cell firing at lags 1/4 of the period of oscillation. Simulations of the oscillations [104, 105] show that travelling waves are thus generated, the intersection of which produces broadband synchrony. In conditions of uniform cortical excitation without strong perturbation from external inputs the exchange of pulses between all cells reaches an equilibrium—that is, a steady-state of symmetrical exchange of signals between excitatory cells at any two positions on the cortex, so that in the oscillating field over sufficient intervals, T,

$$\frac{1}{T}\int_0^T \varphi_e(\mathbf{q},t)-\bar{\varphi}_e\,\mathrm{d}t=\frac{1}{T}\int_0^T \varphi_e(\mathbf{r}',t)-\bar{\varphi}_e\,\mathrm{d}t \tag{18.6}$$

where $\bar{\varphi}_p$ is the time-average presynaptic flux, uniform throughout the cortical field. Since conduction delays are short compared to the period of oscillation, the equality of Eq. (18.6) is generally approached even when T is smaller than the period of oscillation [20], and because there are equal time-lags in both directions of conduction excitatory pulse trains throughout the cortex have maximum correlation at zero lag.

Zero-lag synchronous oscillation thus entails presynaptic pulse synchrony, with a magnitude of presynaptic flux variation that can be defined respectively for individual synapses, and in aggregate, as

$$J^{\mathbf{qr}'}=\left[\frac{1}{T}\int_0^T(\varphi_e^{qr'}(t)-\bar{\varphi}_e)^2\,\mathrm{d}t\right]^{1/2} \tag{18.7}$$

$$J=\left[\frac{1}{T}\int_0^T\int_D\int_D(\varphi_e^{qr'}(t)-\bar{\varphi}_e)^2\,\mathrm{d}\mathbf{q}\,\mathrm{d}\mathbf{r}'\,\mathrm{d}t\right]^{1/2} \tag{18.8}$$

$J^{\mathbf{qr}'}$ is RMS presynaptic flux variation between $\mathbf{q}$ and $\mathbf{r}'$, and J is the aggregate of $J^{\mathbf{qr}'}$ over the cortex. The assumption that selection of neurons that survive apoptosis depends on maximization of J has a series of important consequences. ă

18.2.1 Selection of Scale-Free Small-World Configurations of Neurons

For any given level of cortical excitation, J is greatest for that ensemble of C connected neurons, in which excitatory pulses arrive at dendrites, from all sources at differing distances of separation, as closely in-phase as possible, so as to maximize their summation. Axonal delays, small compared to the period of gamma oscillation,

contribute a phase difference between cell firing at $\mathbf{r}'$ and the arrival of presynaptic pulses at $\mathbf{q}$, of

$$\Delta\Phi^{\mathbf{qr}'} = 2\pi \frac{|\mathbf{q} - \mathbf{r}'|}{P v} \tag{18.9}$$

where P is the period of oscillation. Therefore that ensemble selected by its capacity to maximize presynaptic synchrony must approach minimal total axonal length, $L = \int_D \int_D |\mathbf{q} - \mathbf{r}'| \, d\mathbf{q} \, d\mathbf{r}'$, and minimization of this length also minimizes the metabolic requirements of the axons.

It has been shown generally [21] for all systems of connected elements, the path length in a topological sense is at a minimum where degree distribution follows a power law. As was pointed out in conjunction with Eqs. (18.1)–(18.5), in our idealised neural field, average degree of separation, in the topological sense, increases linearly as metric distance of separation of the cell bodies, so that if L, their total length of axonal connections, is minimal, then the path length in the topological sense is also minimal, and the degree distribution is that of a scale-free, or ultra-small world. Therefore, the connection density between cells versus their metric distance of separation should also be approximated by a power-law distribution. Further, according to Cohen and Havlin [21]

$$L \sim \log \log C \tag{18.10}$$

so the metabolic efficiency of the connection system is further enhanced if the surviving cells are linked into a continuum, as opposed to separate pools of neurons. The number of neighbouring excitatory cells connected to a given excitatory neuron, as a function of distance of separation, is proportional to $2\pi \times f_e^{\mathbf{qr}'}(|\mathbf{q} - \mathbf{r}'|)$ and intracortical axonal trees have approximately exponential density/range relations [15, 84], therefore, because a power function can be fitted exactly by a sum of exponential functions, an ultra-small-world connectivity can be achieved by sets of populations of cells with differing axonal characteristic lengths. During embryogenesis primal cells divide sequentially by layer [78, 86] with differences in growth pattern and characteristic axonal length programmed in sequential cell divisions. For simplicity, we consider only two populations of excitatory cells, with cell bodies partially separated by layer, but with intermingled axonal and dendritic trees, and axonal tree connection probabilities described by

$$f_\alpha^{\mathbf{qR}} = \frac{N_\alpha}{N} 2\pi\lambda_\alpha \exp[-\lambda_\alpha 2\pi |\mathbf{q} - \mathbf{R}|] \tag{18.11}$$

$$f_\beta^{\mathbf{qr}} = \frac{N_\beta}{N} 2\pi\lambda_\beta \exp[-\lambda_\beta 2\pi |\mathbf{q} - \mathbf{r}|] \tag{18.12}$$

$$f_e^{\mathbf{qr}'} = f_\alpha^{\mathbf{qR}} + f_\beta^{\mathbf{qr}}$$

$f_\alpha^{\mathbf{qR}}$ refers to the axonal trees with longest axonal extensions, and $f_\beta^{\mathbf{qr}}$ refers to the axonal trees with short axonal extension, thus $\lambda_\alpha < \lambda_\beta$. $N = N_\alpha + N_\beta$ is the number of synapses received/generated by each cell. Distances from $\mathbf{r}'$ to $\mathbf{q}$ are substituted as $\mathbf{rR}$ to indicate equal distances, $\mathbf{q} - \mathbf{r}$ and $\mathbf{q} - \mathbf{R}$, measured along the axonal trees of the respective populations.

The further defining characteristic of small-world connectivity—the occurrence of connection nodes—emerges as a consequence of the formation of the superficial patch system, as follows.

18.2.2 The Origin of the Superficial Patch System

The two populations of cells and the synapses they give rise to can be referred to as α-cells and synapses, and β-cells and synapses. We first make a provisional assumption (later justified on a species-specific basis) that $N_\beta \gg N_\alpha$, so that α-cells with long-range axons are embedded among much more numerous β-cells. Applying Eqs. (18.11) and (18.12) via Eq. (18.1) to find values of $J^{\mathbf{qr}'}$ in Eq. (18.7) as functions of $|\mathbf{q} - \mathbf{r}, \mathbf{R}|$, shows that

$$\begin{aligned} J^{\mathbf{qr}} &= J^{\mathbf{qR}} \quad \text{if} \quad |\mathbf{q} - \mathbf{r}, \mathbf{R}| = x \\ J^{\mathbf{qr}} &> J^{\mathbf{qR}} \quad \text{if} \quad |\mathbf{q} - \mathbf{r}, \mathbf{R}| < x \\ J^{\mathbf{qr}} &< J^{\mathbf{qR}} \quad \text{if} \quad |\mathbf{q} - \mathbf{r}, \mathbf{R}| > x \end{aligned} \tag{18.13}$$

where $x = -\dfrac{\ln \dfrac{N_\alpha \lambda_\alpha}{N_\beta \lambda_\beta}}{2\pi(\lambda_\beta - \lambda_\alpha)}$.

Consequently (Wright JJ, Bourke PD, 2013, A model for embryogenesis of cortical macrocolumns and superficial patchy connections: consequent neuronal responses at maturity, unpublished manuscript) [106] it can be shown that J (Eq. (18.8)) is at a maximum if β-cells are clustered so they make reciprocal connections at minimum distance and maximum density (β-clusters), and α-cells also form clusters (α-clusters) making reciprocal synaptic connections at distances greater than x, so that they may form multiple patches of synaptic connections, skipping from α-cluster to α-cluster. Also, α-clusters are necessarily placed at the vertices of hexagons tiling the cortical surface, with each hexagon embracing a β-cluster, while reciprocal connections between α- and β-cells occur at cluster margins, over distances approximate to x. Analogy to the superficial patch system in larger-brained species is apparent. See Fig. 18.2.

As noted earlier, hexagonal symmetry of OP and the superficial patch system is an idealization that is roughly approached in some species, while in others it is effectively absent [47]. Since approximation of a power law distribution by two populations of neurons requires $N_\alpha \lll N_\beta$ if $\lambda_\alpha \lll \lambda_\beta$, this case is more

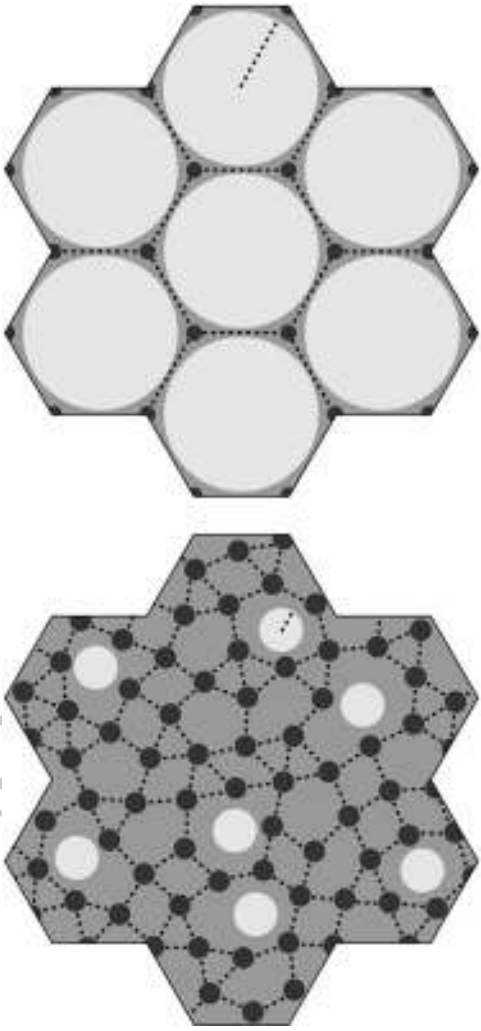

Fig. 18.2 *Pale circles*: neurons coupled by short-range connections. *Black circles*: neurons coupled by long-range patchy connections. *Grey background*: neurons receiving connections of both types. *Dashed lines* are of length $x = -\dfrac{\ln \dfrac{N_\alpha \lambda_\alpha}{N_\beta \lambda_\beta}}{2\pi(\lambda_\beta - \lambda_\alpha)}$. *Top*: $N_\beta \ggg N_\alpha$. *Bottom*: $N_\alpha > N_\beta$

closely approached for larger cortical sizes, and the patchy connection system will have higher orderliness and hexagonal rotational symmetry. If $\lambda_\alpha < \lambda_\beta$ by a small amount, as in animals with small cortical size, then N_β is not necessarily greater than N_α, and an ordered hexagonal structure need not be apparent. Such reduction of the apparent orderliness does not imply the absence of "small world" connectivity, nor imply impairment of function. As a corollary, the same principle of development may apply widely throughout the cortex, as the emergence of clearly defined macrocolumns is determined by the availability of cell types with marked differences in axonal length. This appears to be the case for V1 and S1 (primary somatosensory cortex) in particular, whereas elsewhere, resolution into clear macrocolumns is not so apparent [47].

18.2.3 Self-Organization of Pre-vision Response Properties

Turning from optimization of energy demand of axons, to that of dendrites, we can modify Eq. (18.2) (Wright JJ, Bourke PD, 2013, A model for embryogenesis of cortical macrocolumns and superficial patchy connections: consequent neuronal responses at maturity, unpublished manuscript) [106] to

$$\psi_e^{\mathbf{qr}'}(t) = \Gamma^{\mathbf{qr}'} M_e^{\mathbf{qr}'}(t) * \varphi_e^{\mathbf{qr}'}(t) \tag{18.14}$$

where $\Gamma^{\mathbf{qr}'}$ is the available fraction of the metabolic supply rate needed to attain maximum current flow, and $M_e^{\mathbf{qr}'}(t)$ includes terms for synaptic adaptation and impulse decay, and, most importantly, for presynaptic synergy [96].

Since we have assumed increasing synaptic current in synchronously activated synapses increases the available metabolic supply, the value of $\Gamma^{\mathbf{qr}'}$ must follow that of $\psi_e^{\mathbf{qr}'}(t)$, and as well as inter-cellular competition between assemblies of neurons, we assume competition takes place between adjacent individual synapses arising from the same neuron. Therefore those neurons that survive apoptosis must have found an efficient deployment of resource to the synapses best positioned to maximize the magnitude of synchrony. Since any two adjacent synapses arising from the same pre-synaptic neuron may terminate on the same, or different, post-synaptic neurons, then if they terminate on the same neuron their conditions are essentially identical. If they terminate on different neurons, then the relevant values of $J^{\mathbf{q}}$—their respective synaptic cooperativity with other synapses terminating on the same cell—need not identical—and their competition for resources would lead, via the feedback between $\psi_e^{\mathbf{qr}'}(t)$ and $\Gamma^{\mathbf{qr}'}$, to low synaptic current at one synapse, and high current at the other. Just what the physiological corollary of these opposite high and low-activity states is, and the critical metabolic component for which the synapses compete, we do not specify. A likely, but by no means unique contributing factor is the supply of extracellular calcium [66]. Whatever the critical component(s), the important consequence is that, at synchronous equilibrium, closely situated neurons each receiving synapses from the same cell, must have either high, or low, pulse correlations with each other.

We can term those synapses that are transmitting impulses more strongly near equilibrium "saturated" synapses, and those which are more quiescent, but potentially able to be activated, "sensitive" synapses, and can consider what spatial patterns of saturated connections would best meet the requirement to maximize synchrony. Here a further property of the neural field commented on in relation to Eqs. (18.1)–(18.5)—higher spatial cross-correlation of pulses and field potentials at shorter range—has a decisive impact on the equilibrium pattern of synaptic saturations, in concert with the need for saturated and sensitive synapses to be generated on adjacent post-synaptic neurons. Then, for reasons further argued in (Wright JJ, Bourke PD, 2013, A model for embryogenesis of cortical macrocolumns and superficial patchy connections: consequent neuronal responses at maturity,

unpublished manuscript) [106], the emergent patterns, diagrammed in Fig. 18.3, have the following properties:

(a) Saturated connections within each β-cluster form a re-entrant network analogous to a Möbius strip.
(b) Saturated connections between the α-cluster system and each of the β-clusters form a projection between scales which is homeomorphic, preserving topological identity between scales, and thus mapping a disk to a Möbius strip, and imposing an orientation and chirality on each β-cluster.
(c) Cells in the α-system are linked by saturated synapses.
(d) Saturated connections between β-clusters must project to each of their six neighbors as closely as possible to mirror symmetry, with both saturated and sensitive synapses linking points homologous with respect to position in the α-system—that is to say, points with similar OP as classically measured with low object speeds. The necessarily broken symmetry permits the particular pattern generated to be one of a large set of possible combinations.

Further analogy between the hypothetical α- and β-systems and real anatomical structures can now be drawn. As well as the α-system's congruence with the superficial patch system, the β-systems, each with a dense system of local connections that are centrally spared from patchy connections, are analogous to macrocolumns each centred about an OP singularity. The distribution of OP for lines of orientation $0-\pi$ to angles $0\text{Ű}2\pi$ in pinwheels about a singularity finds analogy in the wrapping of a Euclidean plane onto a Möbius strip. It has also been earlier shown that arrangements of adjacent pinwheels in broken mirror symmetry match classical OP maps [108]. These relations are shown in Figs. 18.3 and 18.4.

Just as OP organization in some species is apparent before eye opening, so too is the organization into OD columns [11, 31]. Explanation of this can be included in the present model by an argument similar to that of Erwin and Miller, who suppose the correlation of cell firing at short distances of separation of V1 cells to be greater than the correlation of visual inputs over a similar distance. This forces a columnar OD organization because of instability—in the present model's terms, the resulting disruption of the synchronous field at equilibrium produced by binocular inputs to the same cells—resolved by formation of columns in Turing patterns.

18.2.4 Consequently, Following Eye-Opening...

After eye opening, visual inputs will provoke ordered departures from the average equilibrium condition.

The emergent map at equilibrium, by which the patchy connections over a part of V1 link to positions within each macrocolumn, can be expressed as 1:1 projection from a disk on a Euclidean plane (the global map), P, to a Möbius strip (the local map), $p^{[2]}$—the square brackets [2] indicating the map's resemblance, if viewed from

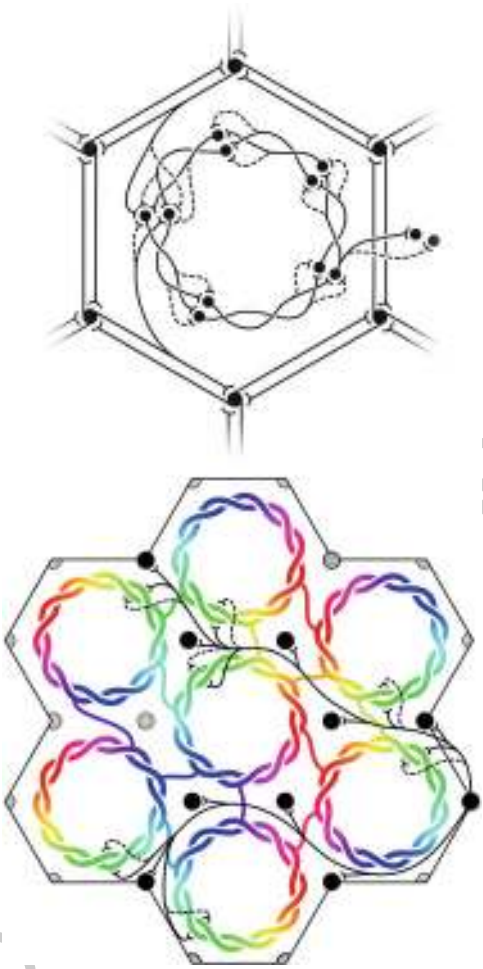

Fig. 18.3 *Top* Equilibrium disposition of saturated and sensitive synapses. *Black circles* represent cell bodies and dendrites. Synapses are indicated as saturated (*solid*) or sensitive (*dashed*) terminations of axons. Reciprocal connections between α-patches (patchy connections) form an hexagonal array. (Other connections, although shown as unidirectional, are also reciprocal.) A representative pair of connections from α-cells to the β-patch is displayed in the upper-and lower aspects of the figure. At the centre of the figure, saturated and sensitive synapses show the network's analogy to a Möbius-strip within a β-patch (macrocolumn). To the right, representative links from the central macrocolumn to cells at homologous positions in neighboring macrocolumns are indicated. *Bottom* "Like to like" saturated patchy connections map the same part of the surrounding cortical field onto homologous cell positions on the Möbius configuration within each macrocolumn, while at short range "like to like" saturated synaptic connections also form between homologous positions between local maps

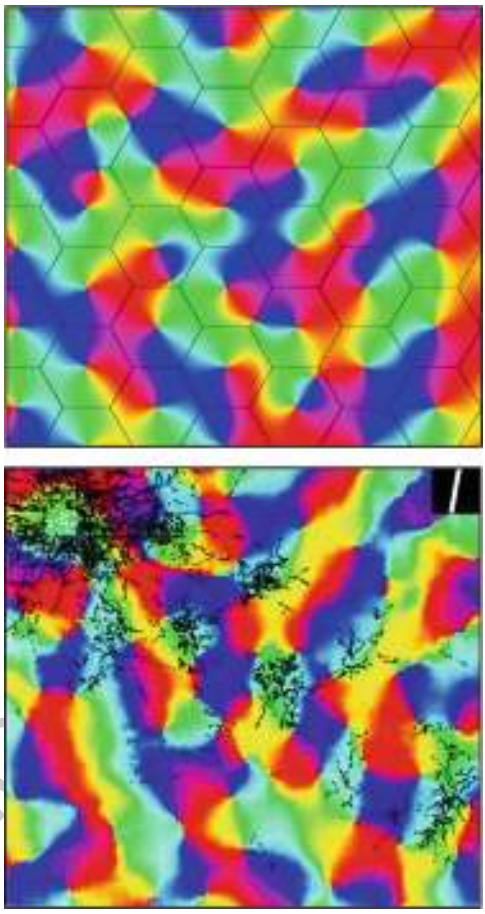

Fig. 18.4 Simulated and real maps of orientation preference in V1, from [108]. *Top*: Simulation. Colours of the spectrum, from *red* to *violet*, represent average OP of V1 neurons for slow-moving visual lines of orientation $0 - \pi$. Adjacent macrocolumns, of diameter approx 300 μm are set within an hexagonal frame (the patch system) with OP forming colour wheels about OP singularities. Orientations and chiralities of the colour wheels are arranged to approach a minimum total of angular disparity from mirror reflection of OP between each macrocolumn and its neighbours. *Bottom*: Real OP. Visualized in the tree shrew by [13]. Superficial patchy connections are demarcated in *black* by a selective stain. Scale of macrocolumns is approximate to that of the simulation

a third dimension, to a 2:1 map formed by squaring a complex vector. In polar coordinates,

$$\mathrm{P}(|\mathbf{R} - \mathbf{C}_j|, \vartheta) \mapsto \mathrm{p}^{[2]}(|\mathbf{r} - \mathbf{C}_j|, \pm\vartheta + \varphi) \tag{18.15}$$

where $\mathbf{C}_j$ is the origin of both P and $\mathrm{p}^{[2]}$ for the j-th local map, and corresponds to the position of the OP singularity in that macrocolumn. ϑ is the polar angle of $\mathbf{R}$, chirality of the local map is indicated by $\pm\vartheta$, and φ is the orientation of the local map relative to the global map. $\vartheta + \varphi$ can be defined on the range $0\text{Ű}2\pi$ in both local and global maps, but is represented with apparent angle doubling in the local map, producing an apparent superposition of angles ϑ and $\vartheta + \varphi$. This describes the form of "contextual" connections [3, 53].

With eye-opening, let $O(\mathrm{P}, t)$ be a visual image projected to V1 by the direct visual pathway. Laterally travelling waves of pulses and local field potentials

transmit that image to each local map with a point to point delay, $\frac{|\mathbf{R}-\mathbf{r}|}{v}$, where v now represents wave speed, so that

$$O(\mathrm{P},t) \mapsto O\left(\mathrm{p}^{[2]}, t + \frac{|\mathbf{R}-\mathbf{r}|}{v}\right) \tag{18.16}$$

Suppose $O(\mathrm{P},t)$ is a segment of the image of a visual line, travelling with uniform velocity, V_x, on the cortical surface, along an x-axis directed toward a macrocolumn with its singularity at $\mathbf{C}_j$, O has a component of its extension on the x-axis, O_x, and an orthogonal component of extension, on the y-axis, O_y. K_x is the dominant spatial frequency of O_x, and K_y is the dominant spatial frequency of O_y. Then the local map projection of O has a transformed spatial frequency in the x-axis but not in the y-axis—i.e.:

$$k_x \propto \frac{v}{v \pm V_x} K_x \tag{18.17}$$

$$k_y \propto K_y\,, \tag{18.18}$$

where k_x, k_y are the spatial frequencies in the local map projection of O, and the sign $\pm$ in Eq. (18.17) depends on whether O is approaching or departing from $\mathbf{C}_j$. That is, O's orientation in the global map is projected to the local map, with Doppler shift, producing an apparent difference in orientation, $\delta\vartheta$;

$$\delta\vartheta = \left|\tan^{-1}\frac{K_y}{K_x} - \tan^{-1}\frac{k_y}{k_x}\right| \tag{18.19}$$

Laterally transmitted contextual signals generally do not trigger cell firing, until the classic receptive field (cRF) is directly stimulated [3, 53] via the visual pathway. The cells that fire are those that reflect the supra-threshold summations of sub-threshold signals conveyed over the contextual, patchy, connections, and the direct pathway. The summation of contextual and direct cRF inputs will act as an impulse causing a transient breakdown of equilibrium, during which synapses that were in both saturated and sensitive state in equilibrium briefly generate substantial synaptic currents (see Fig. 18.5). Action potentials are triggered transiently in surrounding cells. Subsequently there is a restoration toward the equilibrium state on withdrawal of the stimulus. During the breakdown the mapping of activity from the global to the local map becomes

$$O(\mathrm{P},t) \mapsto O\left(\mathrm{p}^{2}, t + \frac{|\mathbf{R}-\mathbf{r}|}{v}\right) \tag{18.20}$$

The change from Eq. (18.16) made by removal of the square brackets from $\mathrm{p}^{[2]}$ represents the breakdown's form, as itself a map from global to local scale, resembling a 2:1 complex-multiplication map, as initially described by Alexander et al. [2].

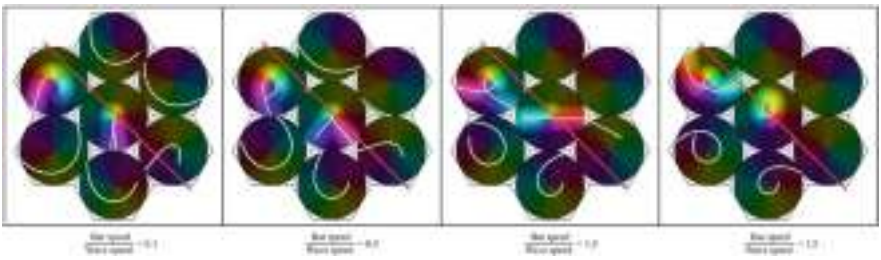

Fig. 18.5 *Red line* is the projection, via the direct visual pathway, of a line in the (monocular) visual field,ăoriented at 45° to the line of passage, andămoving from left to right across a system of 7 macrocolumns in V1. *Green lines* represent the image of the *red line*, transmitted laterally with delay, by patchy (contextual) connections. Bright illumination against the cortical background represents the field of supra-threshold summation of direct pathway and contextual inputs, firing cells with a preferred orientation/velocity/length relation to the *red line*

18.2.5 *Post-natal Effects of Learning, the Spatio-Temporal Filter Model, Dimension Reduction, and "Like To Like" Connections*

Following eye opening, stimuli with regularly repeated spatial and temporal structure reach V1. Exposure to a repeated stimulus will leads to permanent synaptic consolidation of connections, in accordance with physiological versions of the Hebb rule, and the spatio-temporal learning rule [28–30, 72, 73, 96], overlaying any consolidated connections formed in the ante-natal, equilibrium condition. As remarked in the Introduction, Baker and Issa [6] have shown that all V1 response features can be described in terms of six variables—optimal values of orientation preference, spatial frequency preference, and temporal frequency preference, each associated with a Gaussian bandwidth of tuning of the cortical response to these features. These define three hypothetical filter processes. Stimulus variables in the present model have equivalents to those used in the spatio-temporal filter model. These are:

Spatio-temporal model	Present model
Object orientation	Orientation relative to the y-axis defined for Eqs. (18.17) and (18.18)
Object velocity	V_x
Object drift angle	$\tan^{-1}[K_y/K_x]$
Object spatial frequency	$K_x/\cos(\tan^{-1}[K_y/K_x])$
Object temporal frequency	$V_x K_x$

Repeated stimulation with a particular stimulus will therefore lead, under Hebbian learning, to maximization of the response to that stimulus, thus creating an apparent "tuning" of particular neurons to that particular combination of stimulus

features. Thus, the spatio-temporal model can be regarded as a consequence of the present model. Optimization by learning of the parameters for each of the three filters must be competitive between adjacent cells, providing the necessary condition for fitting response maps with continuity and completeness, by dimension-reduction methods [24, 25, 52]. Finally, the consolidation of saturated long-range patchy connections by Hebbian learning would result in mature "like to like" connections.

18.3 Simulations: A Critical Test

A critical test of our model, then, is whether we can reproduce in simulation the results of Basole et al. [8], without appeal to a priori feature-specific responses to orientation, spatial frequency, or temporal frequency, as in the spatio-temporal filter model—the band-width of tuning regarded as a post-natal effect, and not a primary explanation. Equation (18.20) was applied in simulations of an hexagonal array of seven adjacent macrocolumns. Results reported in Fig. 18.6 are for the central macrocolumn of the array of seven. Examples from the array are shown in Fig. 18.5, which shows the orthogonal transformation of apparent OP from the lowest to the highest bar speed for a moving line stimulus oriented at 45° to its line of passage. Again, details of the simulation and controls are given elsewhere (Wright JJ, Bourke PD, 2013, A model for embryogenesis of cortical macrocolumns and superficial patchy connections: consequent neuronal responses at maturity, unpublished manuscript) [106].

18.3.1 Effect of Object Velocity on Apparent Orientation Preference

A moving line in the visual field, relayed by the direct visual pathway to the cRF of each macrocolumn is represented as a red bar. In a single simulation the red bar travelled across the entire hexagonal array from left to right, with constant speed, direction and orientation. The orientation of the red bar to the line of passage is measured as *bar angle* from degrees, where the bar is oriented orthogonally to the direction of travel, to $\pm 90°$, where the bar is oriented in the direction of travel. The lag-transmitted image of the red bar, relayed as subthreshold activation to each macrocolumn via the superficial patch system, is shown in green, with illumination about the zone of subthreshold activation, to indicate that input to the cRF from the direct visual pathway and contextual signals caused triggering of action potentials. The average angle from the macrocolumn singularity to the centers of action potential generation (i.e., all points on the green line with illumination) was calculated at each time-step, and shown as a black arrow, thus indicating the part of the macrocolumn with a response preference (*apparent OP*) for the particular bar

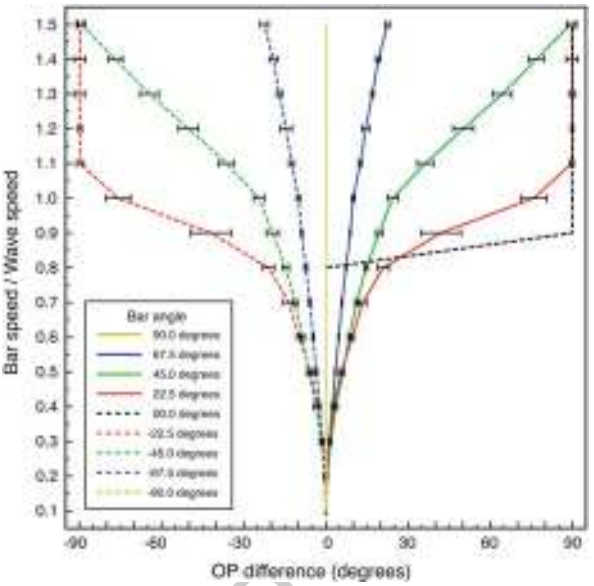

Fig. 18.6 Change in apparent OP, and standard error of the estimate, as a function of bar speed to wave speed, for lines at different orientations to their directions of motion. Bar length 6 units

movement. A change in the sector of the macrocolumn that is maximally stimulated is equivalent to an equal change in the angle of approach of the bar needed to maintain stimulation of the same sector. The black arrow angle was averaged over a window beginning after the red bar had passed the center of the macrocolumn. Combinations of bar-length, orientation of the bar to the direction of movement, and bar speed, were then systematically varied in separate simulations. Their effects on OP, measured at the central local map of the hexagonal group, were obtained as *OP difference*, $\Delta\phi$—a measure of the change in OP as a function of these variables. The *reference OP*, $\phi_0 \in [0, \pi)$, was the OP found at the lowest bar speed applied (bar speed/wave speed = 0.1) and the *apparent OP*, $\phi_1 \in [0, \pi)$, was the OP found at higher speeds.

Systematic results are shown in Fig. 18.6, which graphs OP difference versus bar speed/wave speed, for bar angles to $\pm 90°$, calculated for a bar length of 6 units. Variation of bar length showed progressive lessening of the effect of velocity on OP for greater bar lengths.

For the case of bar-angle 0° (a line oriented orthogonally to its direction of passage, as in classical measurements of OP) no OP difference is seen until, as bar speed approaches wave speed, a 90° change in apparent OP takes place at a single increment in speed. This corresponds to transition to a "motion streak", as object movement blurs resolution in the direction of motion. Increasing OP difference with bar speed at other bar angles is a more gradual development of the same effect—that is, mixing of responses to object speed and to object orientation.

These results match the findings of Basole et al. [8] and are consistent with effects of Doppler shifting of the image transferred from the global to the local map and further selected by the time of activation of the cRF.

To exclude alternative explanations, similar simulations were performed in which contextual (green bar) responses were constrained to occur only with a limited angular response within a macrocolumn. That is, a restricted response to the line, according only to its orientation was imposed, in analogy to conventional models of OP, but with conduction delays of "like to like" fibers included. Then, systematic variation of OP with bar velocity did not occur. A further comparison can be made to the predicted anatomical structure that would emerge if there were no competition for resources between synapses from the same neuron. In that case, OP maps would emerge with any given stimulus orientation represented twice about a singularity—which is not the case.

18.4 Conclusion

From our initial conjecture regarding the evolutionary path to encephalization, we have deduced a model of self-organization in V1 that explains otherwise disparate experimental data, and data which has presented paradoxes to standard explanations. The model's properties also approach a biological optimum, achieving minimum metabolic cost per neuron, minimum total axonal length per connection, and efficient packing, minimizing transmission delays. In effect, the decline of stimulus cross-correlation with increasing distance in visual sensory space, and the corresponding decline of cortical pulse cross-correlation with increasing distance of cell separation, permits development of an internal reference frame for representation of visual events prior to direct visual experience—a *tabula rasa*—upon which subsequent learning can be etched. In the pre-vision state, synaptic couplings at equilibrium are highly orderly, thus offering high information storage capacity, as complex visual correlations become stored by subsequent Hebbian consolidation.

Beyond V1, we speculate that the model may be generally applicable throughout the neocortex. Cortical structure and dynamics, including patch connections, are similar throughout the cortex, and stimulus cross-correlations decline with distance in all sensory modalities—most obviously so for somatic sensation, but also with tone and position in the auditory system. The spatial distribution and intermixing of odour receptors (reviewed by Freeman [32]) implies an analogy even for olfaction. Similar ultra-small world representations might therefore form for all sensory cortices. Although outside primary sensory cortices a similar degree of orderliness of connections is not apparent, that does not exclude the applicability of the model elsewhere, because, as we have seen, the model may be applicable to V1 even in those species which lack strong anatomical ordering, and readily apparent orderliness is a geometrical consequence only for those cortical areas made up of cells with particularly long patch connections.

The principles of the model may also generalize to inter-areal interactions, during embryogenesis. Cortical areas project to and from other areas via cortico-cortical connections, which, because their axons diverge and overlap at their terminations, project substantial parts of one area onto another, and are generally reciprocal between areas [14, 15]. We have argued above that, because co-variance of activity declines with metric distance at both the scale of the patchy connections and within a macrocolumn, a homeotypic mapping between scales can emerge. By similar arguments, sets of macrocolumns at both the lower, V1, level and higher levels, could resonate with, and form preferential connections with, superimposed and overlapping groups at the other level, in accord with the developmental selection requirement to maximize joint synchrony. With the occurrence of eye-opening, Hebbian learning would then begin to overwrite the equilibrium resonance configuration between areas, in analogy to the process at intra-areal level—with the added property of associating concurrent patterns of activity in the V1 macrocolumns. A beginning on defining these reciprocal interrelations has been made elsewhere [106].

Consequently, we may come to an analysis of information flow in the brain's neural networks, in a new way. It has long been known that a macroscopic level, sensory inputs to, and motor outputs from, the cortex are arranged into topographic maps. The present model extends the topographic format to the millimetric scale, and implies that the raw material of cortical information flow is the interaction of spatially organized images. This differs from standard concepts of feature detection, which have dominated conceptions of cortical function since Hubel and Wiesel's famous observations of 1959 [48]. On the Möbius strip, spatial relationships of sensory representations maintain nearest-neighbour relations, and distances from singularities are associated with the distribution of conduction delay from surrounding cortex. Subsequent Hebbian-strengthened connections can bridge points with higher spatio-temporal correlations than accounted for by physical distance of separation in sensory space alone. When the same notion is extended to inter-areal connections, superposition of projections to higher cortical areas permits responses to ever more complex "features" combining stimulus aspects that are separated in visual space. At the ultimate level of expression at the motor cortex, the same organizational model is applicable in the reverse way to that of the sensory cortex—with pyramidal motor neurons substituted for direct visual pathway inputs. The resulting organization is one in which signal flows from sensory inputs to motor cortices could generate organized sensory-motor sequences in response to both externally generated inputs, and to autonomous, internally generated signals [32, 34, 105]. Cortico-cortical connections would permit extension to almost any level of hierarchical complexity—a modular property facilitating the evolution of encephalization.

Acknowledgements The material in this chapter was presented at the First Neural Field Conference, Reading University, UK, (2010), with support of JJW. Special acknowledgement is made of the courage and generosity of Adrienne Wright, in enabling this work, and its presentation on that occasion.

References

1. Albert, M.V., Schnabel, A., Field, D.J.: Innate visual learning through spontaneous activity patterns. PLoS Comput. Biol. **10** (2008). doi:1371/journal.pcbi.1000137
2. Alexander, D.M., Bourke, P.D., Sheridan, P., Konstandatos, O., Wright, J.J.: Intrinsic connections in tree shrew V1 imply a global to local mapping. Vis. Res. **44**, 857–876 (2004)
3. Angelucci, A., Bullier, J.: Reaching beyond the classical receptive field of V1 neurons; horizontal or feedback axons? J. Physiol. (Paris) **97**, 141–154 (2003)
4. Angelucci, A., Levitt, J.B., Lund, J.S.: Anatomical origins of the classic receptive field and modulatory surround field of single neurons in macaque visual cortical area V1. Prog. Brain. Res. **136**, 373–388 (2002)
5. Bahrey, H.L.P., Moody, W.J.: Early development of voltage-gated ion currents and firing properties in neurons of the mouse cerebral cortex. J. Neurophysiol. **89**, 1761–1773 (2002)
6. Baker, T.I., Issa, N.P.: Cortical maps of separable tuning properties predict population responses of complex visual stimuli. J. Neurophysiol. **94**, 775–787 (2005)
7. Barber, M.J., Lichtman, J.W.: Activity-driven synapse elimination leads paradoxically to domination by inactive synapses. J. Neurosci. **19**, 9975–9985 (1999)
8. Basole, A., White, L.E., Fitzpatrick, D.: Mapping of multiple features in the population response of visual cortex. Nature **423**, 986–990 (2003)
9. Basole, A., Kreft-Kerekes, V., White, L.E., Fitzpatrick, D.: Cortical cartography revisited: a frequency perspective on the functional architecture of visual cortex. Prog. Brain Res. **154** (2006)
10. Blakemore, C., Cooper, G. F.: Development of brain depends on the visual environment. Nature **228**, 477–478 (1970)
11. Blakemore, C., Van Sluyters, R.C.: Innate and environmental factors in the development of the kitten's visual cortex. J. Physiol. (Lond.) **248**, 663–716 (1975)
12. Blaschke, A.J., Staley, K., Chun, J.: Widespread programmed cell death in proliferative and postmitotic regions of the fetal cerebral cortex. Development **122**, 1165–1174 (1996)
13. Bosking, W.H., Zhang, Y., Schofield, B., Fitzpatrick, D.: Orientation selectivity and the arrangement of horizontal connections in tree shrew striate cortex. J. Neurosci. **17**(6), 2112–2127 (1997)
14. Boucsein, C., Nawrot, M., Schnepel, P., Aertsen, A.: Beyond the cortical column: abundance and physiology of horizontal connections imply a strong role for inputs from the surround. Front. Neurosci. **5** (2011)
15. Braitenberg, V., Schüz, A.: Anatomy of the cortex: statistics and geometry. Springer, Berlin/New York (1991)
16. Bressler, S.L., Coppola, R., Nakamura R.: Episodic multiregional cortical coherence at multiple frequencies during visual task performance. Nature **366**, 153–156 (1993)
17. Buzás, P., Kovács, K., Ferecskó, A.S., Budd, J.M.L., Eysel, U.T., Kisvárday Z.F.: Model-based analysis of excitatory lateral connections in the visual cortex. J. Comp. Neurol. **499**, 861–881 (2006)
18. Callaway, E.M., Katz, L.C.: Emergence and refinement of clustered horizontal connections in cat striate cortex. J. Neurosci. **10**, 1134–1153 (1990)
19. Carriera-Perpiñán, M.Á., Lister, R.J., Goodhill, G.J.: A computational model for development of multiple maps in primary visual cortex. Cereb. Cortex **15**, 1222–1233 (2005)
20. Chapman, C.L., Bourke, P.D., Wright, J.J.: Spatial eigenmodes and synchronous oscillation: coincidence detection in simulated cerebral cortex. J. Math. Biol. **45**, 57–78 (2002)
21. Cohen, R., Havlin, S.: Scale-free networks are ultra-small. Phys. Rev. Lett. **90**, 058701 (2003)
22. Downes, J.H., Hammond, M.W., Xydas, D., Spencer, M., Becerra, V.M., Warwick, K., Whalley, B.J., Nasuto, S.J.: Emergence of a small-world functional network in cultured neurons. PLoS Comput. Biol. **8**, e1002522 (2012)
23. Durack, J.C., Katz, L.C.: Development of horizontal projections in layer 2/3 of ferret visual cortex. Cereb. Cortex **6**, 178–183 (1996)

AQ2

24. Durbin, R., Mitchison, G.: A dimension reduction framework for understanding cortical maps. Nature **343**, 644–647 (1990)
25. Durbin, R., Willshaw, D.J.: An analogue approach to the travelling salesman problem using an elastic net method. Nature **326**, 689–691 (1987)
26. Eckhorn, R., Bauer, R., Jordon, W., Brosch, M., Kruse, W., Monk, M., Reitboeck, H.J.: Coherent oscillations: a mechanism of feature linking in the in the visual cortex? Biol. Cybern. **60**, 121–130 (1988)
27. Eckhorn, R., Reitboeck, H.J., Arndt, M., Dicke, P.: Feature linking via synchronization among distributed assemblies: simulations of results from cat visual cortex. Neural Comput. **2**, 293–307 (1990)
28. Elliot, T.: Stability against fluctuations: scaling, bifurcations, and spontaneous symmetry breaking in stochastic models of synaptic plasticity. Neural Comput. **23**, 674–734 (2011)
29. Elliott, T., Shadbolt, N.R.: Multiplicative synaptic normalization and a nonlinear Hebb rule underlie a neurotrophic model of competitive synaptic plasticity. Neural Comput. **14**, 1311–1322 (2002)
30. Enoki, R., Hu, Y-L., Hamilton, D., Fine, A.: Expression of long-term plasticity at individual synapses in hippocampus is graded, bi-directional, and mainly pre-synaptic: optic quantal analysis. Neuron **62**, 242–253 (2009)
31. Erwin, E., Miller, K.D.: Correlation-based development of ocularly-matched orientation maps and ocular dominance maps: determination of required input activity structures. J. Neurosci. **18**, 9870–9895 (1998)
32. Freeman, W.J.: Mass Action in the Nervous System. Academic, New York (1975)
33. Freeman, W.J.: Predictions on neocortical dynamics derived from studies in paleocortex. In: Induced Rhythms of the Brain. Birkhäuser, Boston (1991)
34. Freeman, W.J., Quiroga, R.Q.: Imaging Brain Function. Springer, New York/Heidelberg/Dordrecht/London (2013)
35. Gilbert, C.D., Wiesel, T.N.: Morphology and intracortical projections of functionally characteristic neurons in cat visual cortex. Nature **280**, 120–125 (1979)
36. Gilbert, C.D., Wiesel, T.N.: Columnar specificity of intrinsic horizontal and corticocortical connections in cat visual cortex. J. Neurosci. **9**, 2432–2442 (1989)
37. Gray, C.M., König, P., Engel, A.K., Singer, W.: Oscillatory responses in cat visual cortex exhibit intercolumnar synchronisation which reflects global stimulus properties. Nature **388**, 334–337 (1989)
38. Grossberg, S., Olson, S.J.: Rules for the cortical map of ocular dominance and orientation columns. Neural Netw. **7**, 883–894 (1994)
39. Harris, A.E., Ermentrout, G.B., Small, S.L.: A model of ocular column development by competition for trophic factor. Proc. Natl. Acad. Sci. U.S.A. **94**, 9944–9949 (1997)
40. Hashimoto, K., Tsujita, M., Miyazaki, T., Kitamura, K., Yamazaki, M., Shin, H-S., Watanabe, M., Sakimura, K., Kano, M.: Postsynaptic P/Q-type Ca^{2+} channel in Purkinji cell mediates synaptic competition and elimination in developing cerebellum. PNAS **108**, 9987–9992 (2011)
41. Hassenstaub, A., Shu, Y., Haider, B., Krauschaar, U., Duque, A., McCormick, D.A.: Inhibitory postsynaptic potentials carry synchronized frequency information in active cortical networks. Neuron **47**, 423–435 (2005)
42. Hebb, D.: The Organization of Behavior. Wiley, New York (1949)
43. Heck, N., Golbs, A., Riedemann, T., Sun, J-J., Lessmann, V., Luhmann, H.J.: Activity dependent regulation of neuronal apoptosis in neonatal mouse cerebral cortex. Cereb. Cortex **18**, 1335–1349 (2008)
44. Higginbotham, H., Yokota, Y., Anton, E.S.: Strategies for analyzing neuronal progenitor development and neuronal migration in the developing cerebral cortex. Cereb. Cortex **21**, 1465–1474 (2011)
45. Hiramoto, M., Cline, H.: Convergence of multisensory inputs in the xenopus tadpole tectum. Dev. Neurobiol. **69**, 959–971 (2009)

46. Hirsch, J.A., Gilbert, C.D.: Synaptic physiology of horizontal connections in the cat's visual cortex. J. Neurosci. **11**, 1800–1809 (1991)
47. Horton, C.H., Adams, D.L.: The cortical column: a structure without a function. Phil. Trans. R. Soc. B. **360**, 837–862 (2005)
48. Hubel, D.H., Wiesel, T.N.: Receptive fields of single neurones in the cat's striate cortex. J. Physiol. **148**, 574–591 (1959)
49. Issa, P., Rosenberg, A., Husson, T.R.: Models and measurements of functional maps in V1. J. Neurophysiol. **99**, 2745–2754 (2008)
50. James, W.: Psychology (Briefer Course). Holt, New York (1890)
51. Kathuri, N., Lichtman, J.W.: The role of neuronal identity in synaptic competition. Nature **424**, 430 (2003). doi:10.1038/nature01836
52. Kohonen, T.: Self-organized formation of topologically correct feature maps. Biol. Cybern. **43**, 59–69 (1982)
53. Li, W., Their, P., Wehrhahn, C.: Contextual influence on orientation discrimination of humans and responses of neurons in V1 of alert monkeys. J. Neurophysiol. **83**, 941–954 (2000)
54. Linsker, R.: From basic network principles to neural architecture: emergence of spatial opponent cells. Proc. Natl. Acad. Sci. U.S.A. **83**, 7508–7512 (1986)
55. Linsker, R.: From basic network principles to neural architecture: emergence of orientation selective cells. Proc. Natl. Acad. Sci. U.S.A. **83**, 8390–8394 (1986)
56. Linsker, R.: From basic network principles to neural architecture: emergence of orientation columns. Proc. Natl. Acad. Sci. U.S.A. **83**, 8779–8783 (1986)
57. MacLean, P.D.: A triune concept of the brain and behavior. In: Boag, T.J., Campbell, D. (eds.) The Hincks Memorial Lectures, pp. 6–66. University of Toronto Press, Toronto (1973)
58. Marks, G.A., Shaffery, J.P., Okensberg, A., Speciale, S.G., Roffwarg, H.P.: A functional role for REM sleep in brain maturation. Behav. Brain Res. **69**, 1–11 (1995)
59. McGuire, B.A., Gilbert, C.D., Rivlin, P.K., Wiesel, T.N.: Targets of horizontal connections in macaque primary visual cortex. J. Comp. Neurol. **305**, 370–392 (1991)
60. Miller, K.D.: A model for the development of simple cell receptive fields and the ordered arrangement of orientation columns through the activity dependent competition between ON- and OFF-center inputs. J. Neurosci. **14**, 409–441 (1994)
61. Miller, K.D.: Synaptic economics: competition and cooperation in correlation-based synaptic plasticity. Neuron **17**, 371–374 (1996)
62. Mirmiran, M.: The function of fetal/neonatal rapid eye movement sleep. Behav. Brain Res. **69**, 13–22 (1995)
63. Mitchison, G., Crick, F.: Long axons within the striate cortex: their distribution, orientation, and patterns of connection. Brain Pharmacol. **79**, 3661–3665 (1982)
64. Miyashita, M., Tanaka, S.: A mathematical model for the self-organization of orientation columns in visual cortex. NeuroReport **3**, 69–72 (1992)
65. Model, P.G., Bornstein, M.B., Crain, S.M., Pappas, G.D.: An electron microscopic study of the development of synapses in cultured fetal mouse cerebrum continuously exposed to xylocaine. J. Cell Biol. **49**, 362–371 (1971)
66. Montague, P.R.: The resource consumption principle: attention and memory in volumes of neural tissue. Proc. Natl. Acad. Sci. U.S.A. **93**, 3691–3623 (1996)
67. Muir, D.R., Douglas, R.J.: From neural arbours to daisies. Cereb. Cortex **21**, 1118–1133 (2011)
68. Muir, D.R., Da Costa, N.M.A., Girardin, C.C., Naaman, S., Omer, D.B., Ruesch, E., Grinvald, A., Douglas, R.J.: Embedding of cortical representations by the superficial patch system. Cereb. Cortex **21**, 2244–2260 (2011)
69. Newman, J.D., Harris, J.C.: The scientific contributions of Paul D: MacLean. J. Nerv. Ment. Dis. **197**, 3–5 (2009)
70. Obermayer, K., Ritter, H., Schulten, K.: A principle for the formation of the spatial structure of cortical feature maps. Proc. Natl. Acad. Sci. U.S.A. **87**, 8345–8349 (1990)
71. Obermayer, K., Ritter, H., Schulten, K.: A model for the development of the spatial structure of retinotopic maps and orientation columns. IEICE Trans. Fundam. **E75A**, 537–545 (1992)

72. O'Connor, D.H., Wittenberg, G.M., Wang, SS-H.: Dissection of bidirectional synaptic plasticity into saturable unidirectional processes. J. Neurophysiol. **94**, 1565–1573 (2005)
73. O'Connor, D.H., Wittenberg, G.M., Wang, SS-H.: Graded bidirectional synaptic plasticity is composed of switch-like unitary events. Proc. Natl. Acad. Sci. U.S.A. **102**, 9679–9684 (2005)
74. Okomoto, H., Ichikawa, K.: A model for molecular mechanisms of synaptic competition for a finite resource. Biosystems **55**, 65–71 (2000)
75. Paik, S-B., Ringach, D.L.: Retinal origin of orientation maps in visual cortex. Nat. Neurosci. **14**, 919–925 (2011)
76. Papez, J.W.: A proposed mechanism of emotion. Arch. Neurol. Psychiatry **38**, 725–743 (1937)
77. Price, D.J.: The postnatal development of clustered intrinsic connections in area 18 of the visual cortex in kittens. Dev. Brain Res. **24**, 31–38 (1986)
78. Rakic, P.: Specification of cerebral cortical areas. Science **241**, 170–176 (1988)
79. Ringach, D.L.: On the origin of the functional architecture of the cortex. PLoS One **2** e251 (2007)
80. Robinson, P.A., Rennie, C.J., Wright, J.J.: Synchronous oscillations in the cerebral cortex. Phys. Rev. E **57**, 4578–4588 (1998)
81. Rockland, K.S., Lund, J.S.: Intrinsic laminar lattice connections in primate visual cortex. J. Comp. Neurol. **216**, 303–318 (1983)
82. Ruthazer, E.S., Stryker, M.P.: The role of activity in the development of long-range horizontal connections in area 17 of the ferret. J. Neurosci. **16**, 7253–7269 (1996)
83. Schillen, T.B., König, P.: Binding by temporal structure in multiple feature domains of an oscillatory neural network. Biol. Cybern. **70**, 397–405 (1994)
84. Scholl, D.A.: The Organization of the Cerebral Cortex. Wiley, New York (1956)
85. Sherk, H., Stryker, M.P.: Quantitative study of orientation selectivity in visually inexperienced kittens. J. Neurophysiol. **39**, 63–70 (1976)
86. Shi, Y., Kirwan, P., Smith, J., Robinson, H.P.C., Livesey, F.J.: Human cerebral cortex development from pluripotent stem cells to functional cortical synapses. Nat. Neurosci. **15**, 477–486 (2012)
87. Singer, W.: Neuronal synchrony: a versatile code for the definition of relations? Neuron **24**, 49–65 (1999)
88. Sperry, R.W.: Problems Outstanding in the Evolution of Brain Function. James Arthur Lecture on the Evolution of the Human Brain. The American Museum of Natural History, New York (1964)
89. Steriade, M.: Corticothalamic resonance, states of vigilance and mentation. Neuroscience **101**, 243–276 (2000)
90. Swindale, N.V.: A model for the formation of orientation columns. Proc. R. Soc. B. **215**, 211–230 (1982)
91. Swindale, N.V.: A model for the coordinated development of columnar systems in primate striate cortex. Biol. Cybern. **66**, 217–230 (1992)
92. Swindale, N.V.: The development of topography in the visual cortex: a review of models. Netw.: Comput. Neural Syst. **7**, 161–247 (1996)
93. Tanaka, S.: Theory of self-organization of cortical maps: mathematical framework. Neural Netw. **3**, 625–640 (1990)
94. Thomaidou, D., Mione, M.C., Cavanagh, J.F.R., Parnavelas, J.G.: Apoptosis and its relation to the cell cycle in the developing cerebral cortex. J. Neurosci. **17**, 1075–1085 (1997)
95. Traub, R.D., Whittington, M.A., Stanford, I.M., Jefferys, J.G.R.: A mechanism for generation of long-range synchronous fast oscillations in the cortex. Nature **383**, 621–624 (1996)
AQ3 96. Tsukada, M., Fukushima, Y.: A context dependent mechanism in hippocampal CA1 networks. Bull. Math. Biol. (2010)
97. van Ooyen, A.: Competition in the development of nerve connections: a review of models. Netw.: Comput. Neural Syst. **12**, R1–R47 (2001)
98. van Ooyen, A., Willshaw, D.J.: Competition for neurotrophic factor in the development of nerve connections. Proc. R. Soc. Lond. B. **266**, 883–892 (1999)

99. von der Malsburg, C.: Self organization of orientation sensitive cells in the striate cortex. Kybernetik **14**, 85–100 (1973)
100. Whittington, M.A., Faulkner, H.J., Doheny, H.C., Traub, R.D.: Neuronal fast oscillations as a target site for psychoactive drugs. Pharmacol. Ther. **86**, 171–190 (2000)
101. Wiesel, T.N., Hubel, D.H.: Ordered arrangement of orientation columns in monkeys lacking visual experience. J. Comp. Neurol. **158**, 307–318 (1974)
102. Willshaw, D.J., von der Malsburg, C.: How patterned neural connections can be set up by self-organization. Proc. R. Soc. B. **194**, 431–435 (1976)

AQ4

103. Witten, T.A., Sander, L.M.: Diffusion-limited aggregation, a kinetic critical phenomenon. Phys. Rev. Lett. **47**, 1400–1403 (1981)
104. Wright, J.J.: Generation and control of cortical gamma: findings from simulation at two scales. Neural Netw. **22**, 373–384 (2009)
105. Wright, J.J.: Attractor dynamics and thermodynamic analogies in the cerebral cortex: synchronous oscillation, the background EEG, and the regulation of attention. Bull. Math. Biol. (2010)

AQ5

106. Wright, J.J., Bourke, P.D.: On the dynamics of cortical development: synchrony and synaptic self-organization. Front. Comput. Neurosci. **7**, 4 (2013)
107. Wright, J.J., Bourke, P.D., Chapman, C.L.: Synchronous oscillation in the cerebral cortex and object coherence: simulation of basic electrophysiological findings. Biol. Cybern. **83**, 341–353 (2000)
108. Wright, J.J., Alexander, D.M., Bourke, P.D.: Contribution of lateral interactions in V1 to organization of response properties. Vis. Res. **46**, 2703–2720 (2006)
109. Yakovlev, P.I.: Motility, behaviour and the brain; stereodynamic organization and neural co-ordinates of behavior. J. Nerv. Ment. Dis. **107**, 313–335 (1948)
110. Yu, Y-C., He, S., Chen, S., Fu, Y., Brown, K.N., Yao, X-H., Ma, J., Gao, K.P., Sosinsky, G.E., Huang, K., Shi, S-H.: Preferential electrical coupling regulates neocortical lineage-dependent microcircuit assembly. Nature **486**, 113–118 (2012)

AUTHOR QUERIES

AQ1. Please provide e-mail address for the corresponding author.
AQ2. Please provide page range for Refs. [9, 14].
AQ3. Please provide volume number and page range for Refs. [96, 105].
AQ4. Please cite Ref. [103] in text.
AQ5. Unpublished reference "Wright and Bourke (2013)" has been moved to their corresponding citation and the remaining references have been renumbered accordingly. Please check if okay.